

www.acsami.org Research Article

Desalting Plasma Protein Solutions by Membrane Capacitive Deionization

Bharat Shrimant, Tanmay Kulkarni, Mahmudul Hasan, Charles Arnold, Nazimuddin Khan, Abhishek N. Mondal, and Christopher G. Arges*



Cite This: https://doi.org/10.1021/acsami.3c16691



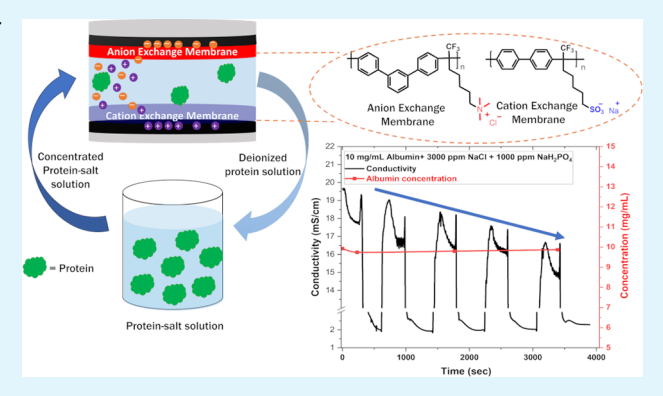
ACCESS I

III Metrics & More

Article Recommendations

s Supporting Information

ABSTRACT: Plasma protein therapies are used by millions of people across the globe to treat a litany of diseases and serious medical conditions. One challenge in the manufacture of plasma protein therapies is the removal of salt ions (e.g., sodium, phosphate, and chloride) from the protein solution. The conventional approach to remove salt ions is the use of diafiltration membranes (e.g., tangential flow filtration) and ion-exchange chromatography. However, the ion-exchange resins within the chromatographic column as well as filtration membranes are subject to fouling by the plasma protein. In this work, we investigate the membrane capacitive deionization (MCDI) as an alternative separation platform for removing ions from plasma protein solutions with negligible protein loss. MCDI has been previously deployed for brackish water



desalination, nutrient recovery, mineral recovery, and removal of pollutants from water. However, this is the first time this technique has been applied for removing 28% of ions (sodium, chloride, and phosphate) from human serum albumin solutions with less than 3% protein loss from the process stream. Furthermore, the MCDI experiments utilized highly conductive poly(phenylene alkylene)-based ion exchange membranes (IEMs). These IEMs combined with ionomer-coated nylon meshes in the spacer channel ameliorate Ohmic resistances in MCDI improving the energy efficiency. Overall, we envision MCDI as an effective separation platform in biopharmaceutical manufacturing for deionizing plasma protein solutions and other pharmaceutical formulations without a loss of active pharmaceutical ingredients.

KEYWORDS: membrane capacitive deionization, poly(phenylene alkylene) ion exchange membranes, plasma proteins, albumin, electrochemical separations

■ INTRODUCTION

Proteins are important macromolecules for all forms of life as they influence cell metabolism, the immune system of living organisms, and perform other important bodily activities. Human serum albumin (HSA) is the most abundant protein in the human body and has many applications in medical fields such as replacing lost albumin in patients with hypoalbuminemia, treating hypovolemia, as a part of some diagnostic imaging kits, and as a supplement for cell culture. HSA is one type of plasma-derived protein used for numerous therapies. In addition to HSA, there are other plasma proteins, such as globulins/immunoglobulins and fibrinogen, that are also used as therapies to treat a variety of diseases and medical conditions. ^{5–7}

The processing of plasma protein formulations for medical use entails multiple separation units such as chromatography, filtration, and dialysis. One notable challenge in the separation process is the removal of inorganic salt ions from the plasma protein process stream without diluting or losing the plasma protein from the process stream. Ion-exchange column chromatography using resin particles, dialysis, gel filtration, and

ultra/diafiltration membranes are often deployed to remove excess salt, such as sodium chloride and phosphate salts from the process stream containing the plasma protein. However, these approaches are either time-consuming, increase sample volumes, or the membranes and resins used are prone to fouling by the proteins. Protein fouling, in particular, is catastrophic, as it is the most valuable material in the stream and any loss increases manufacturing costs. It is also worth mentioning that ion-exchange chromatography necessitates chemicals for regenerating the resin bed, and this leads to process waste and a longer separation process. Devising a separation unit that can directly deionize the protein solution without concern for protein fouling while also having short

Received: November 7, 2023 Revised: February 6, 2024 Accepted: February 14, 2024



Table 1. IEM Properties

membrane type	thickness (μm)	IEC (mequiv g^{-1})	WU (%)	SR (%)	κ (mS/cm) in DI water	ASR (ohm cm ²)
Fumasep CEM	75	1.5	17	7	10.0	0.8
Fumasep AEM	75	1.3	15	4	4.4	1.7
BPSA CEM	30	2.4	26	9	29.8	0.1
m-TPN1 AEM	41	2.1	20	5	14.7	0.3

down times will benefit plasma protein manufacturing operations.

Electrodialysis (ED), electrodeionization (EDI), and capacitive deionization (CDI)/membrane capacitive deionization (MCDI) are commercial electrochemical separation processes used for removing ions from solutions. ¹⁹ In addition to being deployed for desalination, they have also been used for heavy metal ion removal, organic acid removal, nutrient recovery, and recovery of critical minerals.²⁰⁻²⁴ Recent developments have seen these electrochemical platforms being adopted for deionization of small organic molecules such as lactic acid, pcoumaric acid, itaconic acid, and so forth as well as macromolecules (proteins, globulins, etc.) from biochemical feed streams. ^{25–29} In the context of deionizing plasma protein solutions, EDI is ill-suited because the unit features ionexchange resins that are prone to fouling. In practice, ED will have its polarity flipped, known as electrodialysis reversal (EDR), to prevent ion-exchange membrane fouling by surfactants—which are charged macromolecules that have some resemblance to proteins. ED, the most mature electrochemical deionization process, suffers from severe Ohmic losses in the process stream when a good portion of the ions are removed. Furthermore, ED faces challenges, such as the back diffusion of ions and water crossover. In this process, ionexchange membranes confront a concentrated solution on one side and a diluted solution on the other, resulting in the back diffusion of ions from the concentrated to the diluted stream.³⁰ The water crossover issue in electrodialysis is attributed to osmosis and electro-osmosis. This phenomenon has a dual impact: (1) the desalination of the water stream is less efficient due to undesired water removal, and (2) the concentration of the brine stream is less effective due to the undesirable crossover of water molecules into the brine stream.³¹ Traditionally, in electrodialysis, addressing these challenges involves sacrificing the ionic conductivity of membranes by using thicker or crosslinked membranes to prevent water crossover between the dilute and concentrate chambers.³² The drawback of water crossover in ED lies in the unfavorable energy expenditure required for transporting water through IEMs, as well as an increase in brine concentration due to reduced dilution. However, the water crossover challenge has yet to be observed in MCDI.

Compared to ED, CDI and MCDI are less mature electrochemical deionization platforms. They have attracted attention in recent years for deionizing brackish water streams because energy can be recovered during the electrode regeneration step resulting in a low specific-energy consumption for desalination.³³ Like EDR, CDI and MCDI flip the cell polarity to regenerate the electrodes. This polarity reversal would make CDI and MCDI less amenable to fouling by charged macromolecules such as proteins. MCDI differs from CDI because it has ion-exchange membranes (IEMs) that cover the porous electrodes to prevent co-ion adsorption and to promote current utilization during deionization.³⁴

In the CDI and MCDI processes, a cell voltage difference is applied to two porous electrodes. An anion exchange membrane

(AEM) covers the positively biased electrode in MCDI to remove anions from the process stream, while a cation exchange membrane (CEM) covers the negatively biased electrode to remove cations. The removed ions are stored in the electrochemical double layer of the porous, activated carbon electrodes. After a period of deionization, the direction of the electrical current for the cell is reversed to regenerate the porous electrodes. This discharge step leads to ion removal from the electrodes (i.e., regeneration) and a more concentrated salt solution. Notably, MCDI, like other electrochemical deionization platforms, operates under mild ambient conditions, whereas distillation and membrane filtration, which are the conventional separation platforms used in chemical processes, necessitate high pressure and elevated temperatures. These extreme conditions can damage the protein in solution.

In this work, we investigated MCDI for deionizing HSA solutions containing dissolved sodium chloride (NaCl) and monosodium dihydrogen phosphate (NaH2PO4). Prior to performing the deionization experiments with HSA, we examined the MCDI performance at different NaCl and/or NaH₂PO₄ feed concentrations with highly conductive poly-(phenylene alkylene) IEMs and porous meshes coated with poly(phenylene alkylene) ionomers. These aromatic polymers possess a backbone consisting entirely of C-C bonds (i.e., no heteroatom linkages) showcasing remarkable stability and efficacy in both fuel cells and electrolyzers.³⁷ Other notable attribute includes high ionic conductivity, good solubility, and scalable manufacturing. Our previous work showed that IEMs with $\geq 4 \times$ reduction in area specific resistance (ASR) resulted in a 2× increase in the energy-normalized adsorbed salt (ENAS inversely commensurate to specific energy consumption). Hence, IEMs that are more conductive and thinner improve the energy metrics of MCDI.³⁸ In a subsequent report, we used ionomer-coated nylon meshes placed in the spacer channel (where the process stream passes through) to augment the process stream ionic conductivity.³⁹ This resulted in $\geq 2\times$ increase in the ENAS values when compared to a MCDI process that did not have a porous ionic conductor. The ionomer materials deployed in our previous work used poly(arylene ether) backbones. These materials have lower ionic conductivity when compared to the more recent poly(phenylene alkylene) ionomers developed for fuel cell and electrolysis applications.40-42 Here, we show that the highly conductive poly-(phenylene alkylene) ionomers used as IEMs and porous ionic conductors are effective for deionizing NaCl and NaH2PO4 salt solutions (single salt in water or a mixture of salts in water) at different concentrations (up to 8 g L⁻¹). Additionally, we also show that the said ionomer materials implemented in MCDI are effective for deionizing salt-plasma protein mixtures with 18-28% salt removal while demonstrating negligible loss (<3%) of albumin from the process stream. Overall, MCDI with advanced ionomer materials is an effective deionization platform for plasma protein solutions.

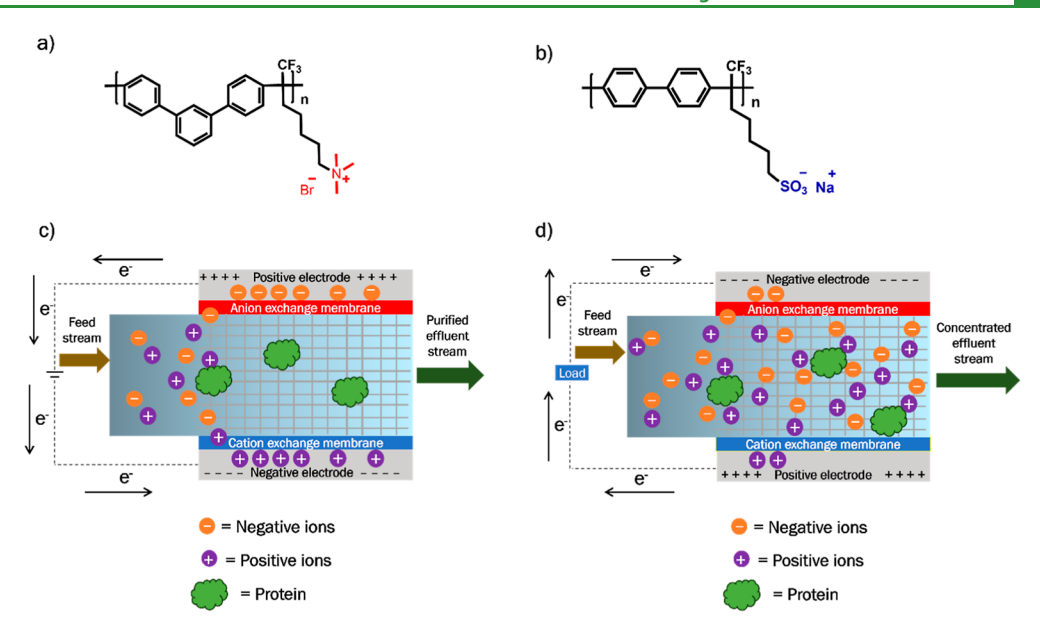


Figure 1. Chemical structures of the (a) AEM and (b) CEM. MCDI process flow schemes for (c) charge/deionization cycle and (d) discharge/regeneration cycle.

RESULTS AND DISCUSSION

Synthesis and Properties of IEMs. IEMs for MCDI should display high ionic conductivity while also demonstrating low water uptake (WU) and strong mechanical properties.⁴³ High water uptake leads to excessive swelling of membranes within the cell, jeopardizing mechanical properties. The poly-(phenylene alkylene) IEMs in this work have excellent ionic conductivity because of their high IEC values (2.1-2.4 mequiv g⁻¹, Table 1). Furthermore, the all-carbon, aromatic repeat units of m-terphenyl and biphenyl in these ionomers suppress water uptake and swelling (≤26% WU and ≤9% SR) (Table 1).^{40,44} The chemical structures of the poly(phenylene alkylene) AEM and CEM are shown in Figure 1. There has only been one report investing the class of poly(phenylene alkylene) ionomers for MCDI. 45 This recent article investigated poly(fluorene) backbone anion exchange ionomer and cation exchange ionomer variants and compared the electrode salt capacity and charge efficiency of CDI and MCDI with commercial ASTOM IEMs, and MCDI where the poly(fluorene) ionomers coated the porous electrodes. The article examined only deionization of a single concentration of 500 ppm of NaCl in water.

The poly(phenylene alkylene) IEMs used in this work were prepared by superacid-catalyzed polymerization of aromatics (m-terphenyl and biphenyl) and 7-bromo-1,1,1-trifluorohexane-2-one as depicted in Schemes S1 and S2. The trimethylammonium group was introduced into the AEM by the Menshutkin reaction of the alkylated bromide functionality in *m*-TPBr with trimethylamine. The CEM was prepared by two different synthetic routes. In the first route, biphenyl backbone with alkylated bromide functionality (BPBr) was reacted with potassium thioacetate followed by oxidation of the thioacetate group to a sulfonic acid group using hydrogen peroxide in formic acid. After the heterogeneous oxidation reaction, CEM was not soluble in any solvent. In the second synthetic route approach, the thioacetate group was oxidized to sulfonic acid group using m-chloroperbenzoic acid (m-CPBA) to obtain soluble cation exchange ionomer. The ¹H NMR spectra substantiating the polymer structures are provided in Figures S1-S5. The Mn values of the poly(phenylene alkylene) precursors with terminal

bromo groups ranged from 45 to 78 kDa. These values were determined by GPC.

Most MCDI studies deploy commercially available IEMs used in electrodialysis. For benchmarking purposes, we compared the ionic conductivity, water uptake, and swelling ratio of the poly(phenylene alkylene) IEMs against commercially available IEMs from Fumatech. The poly(phenylene alkylene) IEMs showed 3× higher ionic conductivity (or more) than the Fumasep IEMs (Table 1). Because the poly(phenylene alkylene) IEMs are almost 2× thinner than the Fumatech IEMs, their ASR values are at least 6× lower. The poly-(phenylene alkylene) IEMs' water uptake (Table 1) is slightly higher than the Fumasep IEMs (20–26% versus 15–17%), but the swelling ratios between the two classes of the IEMs are about the same. The poly(phenylene alkylene) backbones were effective for suppressing the water uptake. The high ionic conductivity and low swelling ratio of the poly(phenylene alkylene) IEMs make them good candidates for MCDI.

MCDI Experiments without HSA. Prior to deionizing plasma protein solutions, initial experiments were performed to test how effective poly(phenylene alkylene) IEMs and porous ionic conductors are for deionizing NaCl and NaH₂PO₄ feed solutions. The first set of experiments compared MCDI performance with 250 ppm of NaCl feed using poly(phenylene alkylene) IEMs and Fumatech IEMs. Then, MCDI experiments were performed with poly(phenylene alkylene) IEMs with a porous ionic conductor in the spacer channel and no porous ionic conductor in the spacer channel with 250 ppm of NaCl_{aq} feeds. These experiments were performed with low NaCl feed concentrations to accentuate how the ASR values of the IEMs and porous ionic conductors affect MCDI energy use.

After establishing that poly(phenylene alkylene) IEMs and porous ionic conductors were more effective than Fumatech IEMs and MCDI with no porous ionic conductors, a series of MCDI experiments were performed with 8000 ppm of NaCl and 6000 ppm of NaH₂PO₄. These experiments used poly(phenylene alkylene) IEMs and examined the scenarios with a porous ionic conductor and no porous ionic conductor. It is important to note that most MCDI studies examine model

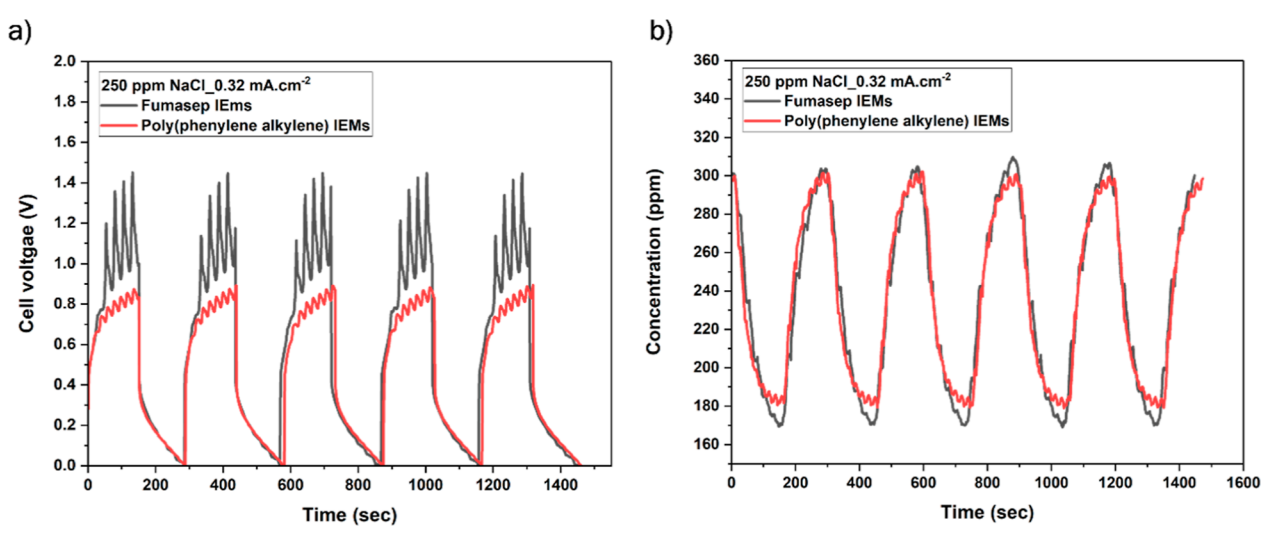


Figure 2. (a) Cell voltage versus time and (b) effluent NaCl concentration versus time for charge—discharge cycling at a constant current density of ± 0.32 mA cm⁻² in MCDI for 250 ppm of NaCl feed with Fumasep IEMs (black) and poly(phenylene alkylene) IEMs (red).

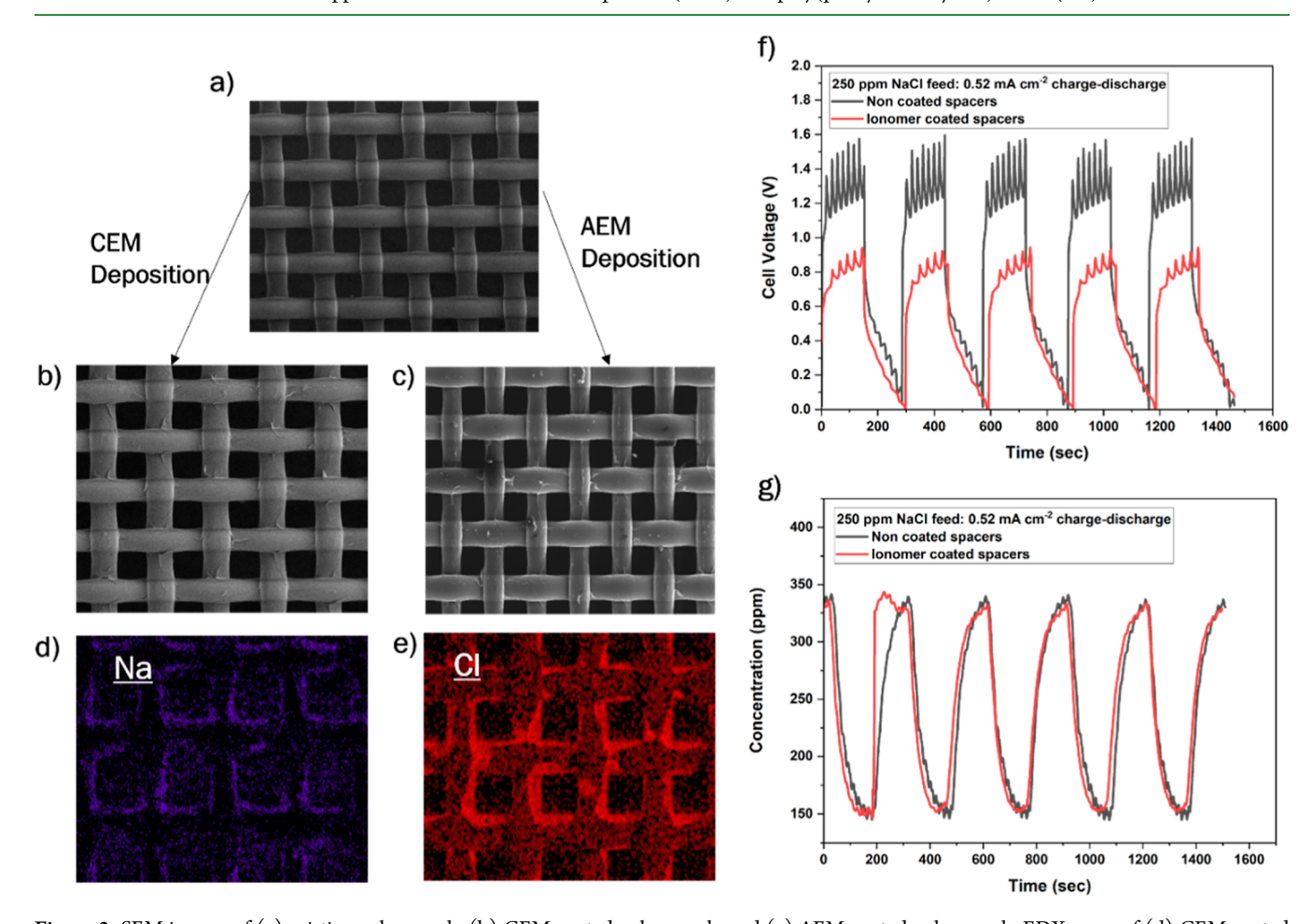


Figure 3. SEM images of (a) pristine nylon mesh, (b) CEM-coated nylon mesh, and (c) AEM-coated nylon mesh. EDX maps of (d) CEM-coated nylon mesh, and (e) AEM-coated nylon mesh. (f) Cell voltage versus time and (g) effluent NaCl concentration profile for charge—discharge cycles in MCDI for 250 ppm of NaCl with noncoated (black) and ionomer-coated (red) nylon meshes in the spacer channel. The EDX map of the CEM-coated nylon mesh traces sodium (Na⁺ counterions in the cation exchange ionomer), represented by the purple color in (d). Similarly, the EDX map of the AEM coated mesh tracks chlorine (Cl⁻ counterions in the anion exchange ionomer), as represented by the red color in (e).

brackish water feeds (≤5000 ppm of NaCl). However, the salt concentration in plasma protein solutions is often higher than brackish water streams.

Figure 2a,b shows charge—discharge cell voltage and effluent concentration curves for 250 ppm of NaCl feed for MCDI featuring poly(phenylene alkylene) IEMs and Fumatech IEMs. Table S1 provides the salt removal efficiency (SRE), Coulombic

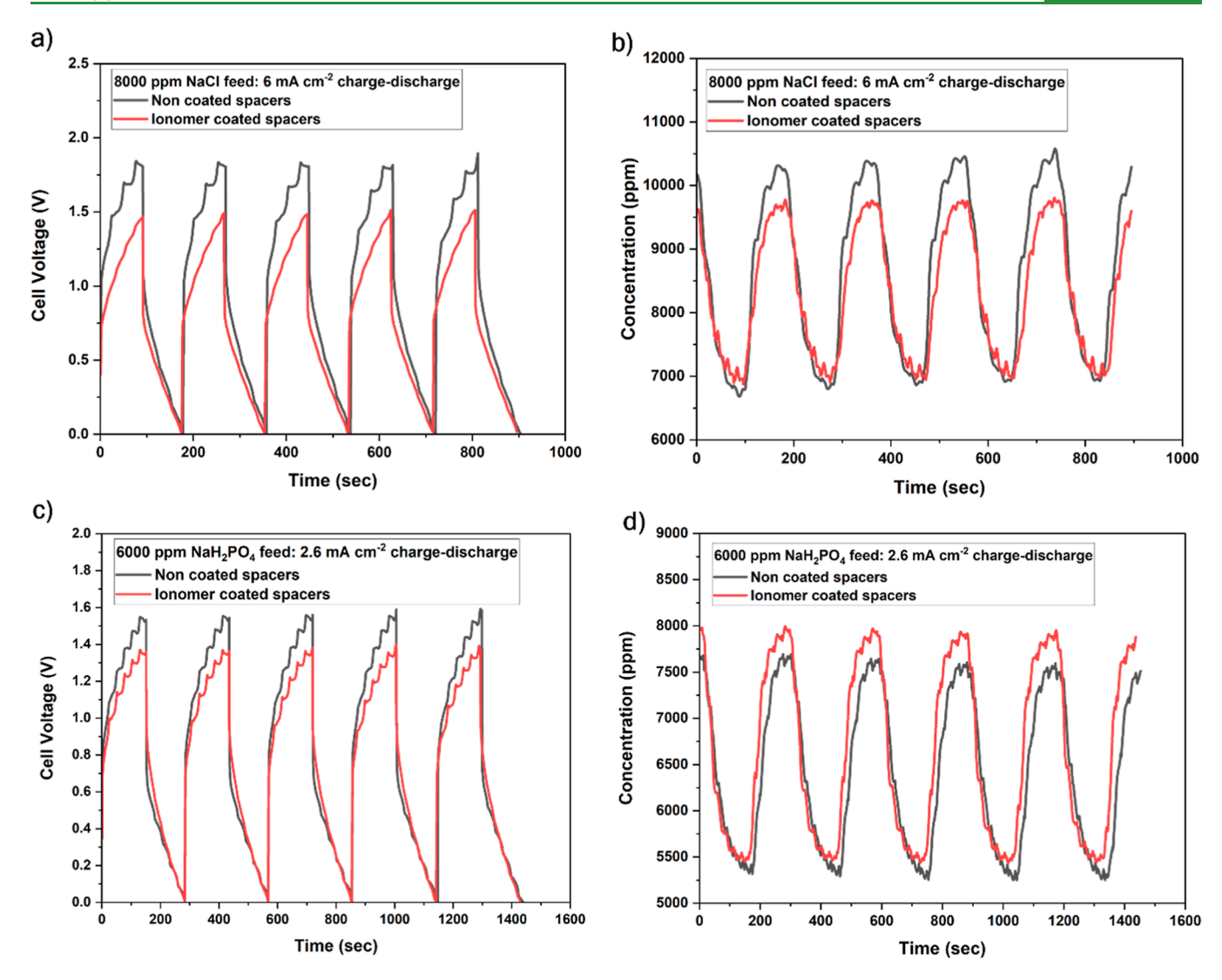


Figure 4. (a) Cell voltage versus time and (b) effluent NaCl concentration versus time for charge—discharge cycles in MCDI for 8000 ppm of NaCl with noncoated (black) and ionomer coated (red). (c) Cell voltage versus time and (d) effluent NaH₂PO₄ concentration versus time for charge—discharge cycles in MCDI for 6000 ppm of NaH₂PO₄ with noncoated (black) and ionomer coated (red).

efficiency (CE), and average salt absorption rate (ASAR) from the MCDI experiments with this salt feed concentration and at a constant current density (0.32 mA cm⁻²). Because the MCDI unit was operated under constant current, the SRE, CE, and ASAR were relatively the same between experiments with the different types of IEMs. However, there was a significant difference in the cell voltage curves between the two configurations. The adoption of the more conductive poly-(phenylene alkylene) IEMs reduced the cell voltage by 300 mV during the charge step. During the MCDI experiments, EIS was performed to assess differences in the high frequency resistance (HFR). From the HFR values shown in the Nyquist plot (Figure S8), the cell HFR was reduced by 24% when using the poly(phenylene alkylene) IEMs as opposed to the Fumatech IEMs. The HFR values (also known as R_s) are provided in Table S3. The energy recovery values of the MCDI unit with a 250 ppm feed for the two different sets of IEMs as well as the energy use upon charging and discharging are provided in Table S1. From the control case of MCDI with no porous ionic conductor and using electrodialysis IEMs (Fumasep), the ENAS was 21% higher when using poly(phenylene alkylene) IEMs and no porous ionic conductor. The ENAS value is inversely commensurate with the HFR (i.e., a reduction in HFR yields a larger ENAS value).

The next set of experiments compared MCDI performance with porous ionic conductors in the spacer compartment and with no porous ionic conductor in the spacer compartment with poly(phenylene alkylene) IEMs. As the process stream becomes deionized, the Ohmic resistance in the spacer compartment becomes substantial and hinders the energy efficiency of the MCDI process. We coated poly(phenylene) anion exchange ionomer on one sheet of nylon mesh via aerosol spray deposition to a loading of 2.4 mg cm⁻². Then, a poly(phenylene) cation exchange ionomer on an identical bare nylon sheet was deposited until a loading of 2.4 mg cm⁻² was attained. Figure 3a-e presents electron micrographs of the porous nylon mesh with and without ionomer coatings. This figure also gives EDX images substantiating the presence of the sodium and chloride counterions in the ionomer coated nylon meshes before running MCDI experiments. Figure 3f,g shows the MCDI chargedischarge cell voltage and effluent concentration curves for 250 ppm of NaCl with noncoated and ionomer-coated meshes in the spacer channel. Nylon meshes coated with highly conductive poly(phenylene alkylene) ionomers reduced the cell voltage by

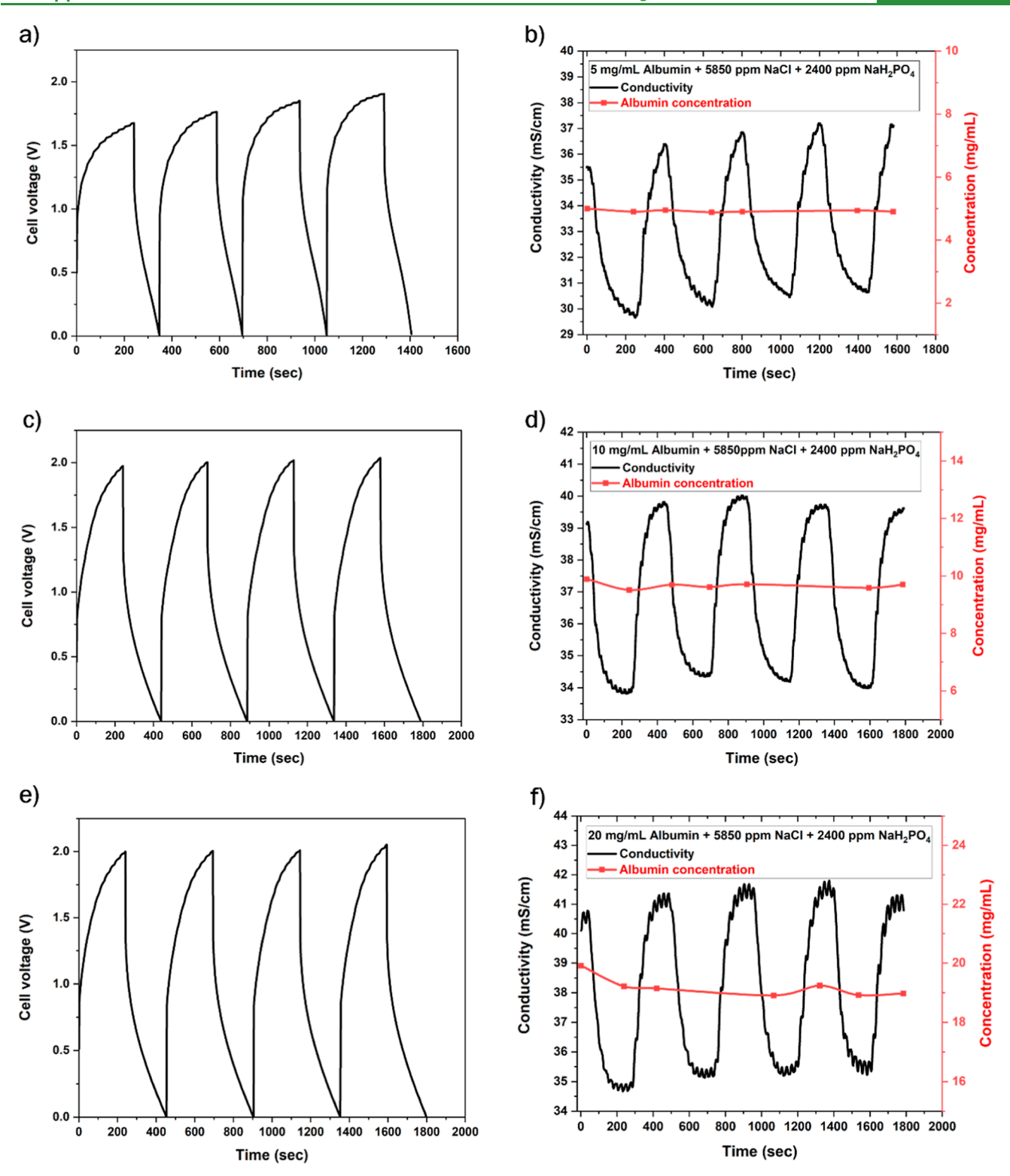


Figure 5. Cell voltage versus time and effluent conductivity versus time and albumin concentration vs time for charge—discharge cycling at a constant current density of ± 3 mA cm⁻² in MCDI for the following albumin concentration in the feed: (a,b) 5 mg/mL HSA, (c,d) 10 mg/mL HSA, and (e,f) 20 mg/mL HSA.

500 mV when operating at a constant current of 0.52 mA cm⁻². A higher current density was used in the deionization and electrode regeneration step in these experiments because the poly(phenylene alkylene) IEMs reduced the cell's Ohmic resistance. The SRE and ASAR values, reported in Table S2, were identical for both configurations (ionomer coated nylon meshes and noncoated nylon meshes) because both experi-

ments were operated at the same current density. Table S2 also provides the energy use and recovery values for these two configurations. Figure S9 provides the Nyquist plot attained from the EIS during MCDI experiments. The porous ionic conductors reduced the HFR by 22%. The ENAS values for MCDI with 250 ppm of NaCl feed and operating at 0.52 mA cm⁻² increased by 40% when using a porous ionic conductor.

The ENAS values for the MCDI experiments with and without porous ionic conductors and poly(phenylene alkylene) IEMs with 250 ppm of NaCl feeds are given in Table S2.

After establishing the effectiveness of poly(phenylene alkylene) ionomer materials for MCDI, the next set of experiments investigated deionization of higher salt feed concentrations such as 8000 ppm of NaCl and 6000 ppm of NaH₂PO₄ solutions. At the onset of the experiments, it was unclear if the porous ionic conductors would still be effective for augmenting spacer channel conductivity given the higher feed concentration and performing a single-pass MCDI assessment. Figure 4a-d presents the MCDI voltage versus time and effluent concentration versus time for 8000 ppm of NaCl feeds and 6000 ppm of NaH₂PO₄ feeds. The MCDI operating parameters with the said feed solutions are provided in Table S2. The SRE decreased from mid-50 to 28 to 33% when increasing feed concentration from 250 to 8000 ppm of NaCl and 6000 ppm of NaH₂PO₄. The drop in the SRE arises from the larger amount of salt in the feed while keeping the cell active area constant. A bigger cell area would provide a large SRE. When operating MCDI at 6 mA cm⁻² for the 8000 ppm of NaCl feed with or without a porous ionic conductor, it is worth noting that the change in effluent concentration was 2500-3000 ppm for 25 cm² active area. Although an 8000 ppm of NaCl feed solution is sent through the MCDI, the traces in Figure 4b shows an apex value of 10,000 ppm of NaCl. This occurs because the first three charge-discharge cycles are excluded as part of a cell conditioning protocol in our lab. During the electrode regeneration/discharge cycle step, the salt adsorbed in the porous electrode is removed and added to the 8000 ppm of NaCl feed leading to a brine solution of about 10,000 ppm.

It is worth noting that most MCDI papers examining new electrode or IEM materials use synthetic brackish water streams mostly composed of NaCl \leq 5000 ppm in deionized water. ⁴⁶ However, the plasma protein solutions contain a lot more NaCl, and hence, we demonstrated that the poly(phenylene alkylene) IEMs are effective for deionizing higher concentration salt feeds in MCDI. We anticipate that a greater SRE is possible by using a larger active area with additional cells in series. Another pathway for more salt removal involves using two liquid streams: (1) a recirculating plasma protein stream that is being deionized and (2) a waste brine stream that is used for electrode regeneration. This latter approach will be discussed in further detail later. Finally, we also wish to point out that the nylon meshes coated with poly(phenylene alkylene) ionomer were effective for augmenting spacer channel ionic conductivity with NaCl concentrations of 6000 to 10,000 ppm resulting in about a 300 mV lower cell voltage when running the unit at 6 mA cm⁻².

Plasma protein formulations often contain phosphate salts as buffering agent. There have been few reports on using MCDI to remove phosphate anions from aqueous streams—mostly in the context of phosphorus recovery from fertilizer runoff. Our first experiments attempting to deionize NaH₂PO₄ aqueous solutions led to poor SRE values at various cell voltages (as high as 2 V). This observation is in line with another literature report using a high cell voltage to deionize phosphate solutions. The problem was remediated by letting a 250 ppm of NaH₂PO₄ solution sit in the spacer compartment of an assembled MCDI cell with poly(phenylene alkylene) IEMs with and without a porous ionic conductor for 12–16 h before running deionization experiments. This conditioning step allowed us to attain SR values of 28% while maintaining the cell voltage below 1.5 V when using a 6000 ppm of NaH₂PO₄ feed and operating the

MCDI at 2.6 mA cm⁻². Figure 4c,d presents the cell voltage versus time and the NaH₂PO₄-effluent concentration versus time during the charge-discharge cycling in the cell. Similar to the 8000 ppm of NaCl MCDI experiments, it is important to note that the discharge cycle during MCDI leads to a peak effluent concentration of 7600 to 8000 ppm of NaH₂PO₄. Finally, a porous ionic conductor in the MCDI setup reduced the cell voltage by 200 mV when deionizing 6000 ppm of NaH₂PO₄ at 2.6 mA cm⁻². The lower cell voltage drops when using a porous ionic conductor for 6000 ppm of NaH2PO4 compared to using a porous ionic conductor with NaCl feeds was attributed to the lower ionic mobility of the dihydrogen phosphate anion over the chloride anion. Figure S11 gives the Nyquist plot for deionizing 6000 ppm of NaH₂PO₄ at 2.6 mA cm⁻² with and without porous ionic conductors. The HFR value decreased by 5% when ionomer-coated spacers were used. Table S2 reports the SRE, energy recovery, and ENAS values for deionizing 6000 ppm of NaH2PO4 feed solutions. Overall, Figure 4 demonstrates that poly(phenylene alkylene) ionomer materials, used as IEMs and coatings on nylon meshes in the spacer channel, are effective for deionizing process streams with over >5 g L⁻¹ salt solutions.

MCDI Experiments with HSA-Salt Solutions. The final set of experiments tested the extent of plasma protein solution deionization while concurrently assessing if any HSA was lost during the deionization process. Figure 5a-f reports the effluent stream conductivity during charge—discharge cycling in MCDI with a feed stream of 5800 ppm of NaCl mixed, 2400 ppm of sodium phosphate, and 5, 10, or 20 mg mL⁻¹ of HSA. We test this HSA concentration range as it corresponds to a model process stream in biopharmaceutical manufacturing. Plus, we also wanted to assess if higher concentrations of HSA would exacerbate fouling.

Figure 5b,d,f shows a 18-20% drop in effluent stream ionic conductivity while showing 1 to 3% HSA loss—a negligible and acceptable loss. In previous MCDI experiments with a single salt in the feed stream, an ionic conductivity calibration curve could be used to determine the effluent stream concentration. However, ionic conductivity cannot discriminate between the different concentrations in ions. Inductively coupled plasmaoptical emission spectrometry (ICP-OES) was used to quantify the amount of sodium and phosphate removed from the process stream. The difference between the amount of phosphate removed and sodium removed was equivalent to the amount of chloride removed. Tables S5-S7 report the amount of sodium, phosphate, and chloride removed upon the charge-discharge cycles that correspond to Figure 5a-f. UV-vis was used to assay the HSA concentration in the effluent stream at various time points during the charge—discharge cycling. Figure S14 provides the raw UV-vis data for collected and diluted process stream solutions. Overall, there is negligible change in the absorption peak affiliated with HSA. Moreover, there are no shifts in the absorbance spectrum of the first sample (collected at the start of the deionization experiment) and the subsequent samples (collected during the experiment). Albumin is stable if the solution does not see a pH value below 4.⁵⁰ Our previous work showed that maintaining our cell voltage <2 V kept the pH above 4. Additionally, we observed no aggregates in the effluent stream during MCDI with HSA feeds. Aggregates would occur if the pH was too low. For these reasons, we infer that albumin remains stable during charge-discharge cycling in MCDI. Overall, Figure 5 conveys successful salt removal from HSA solutions in a

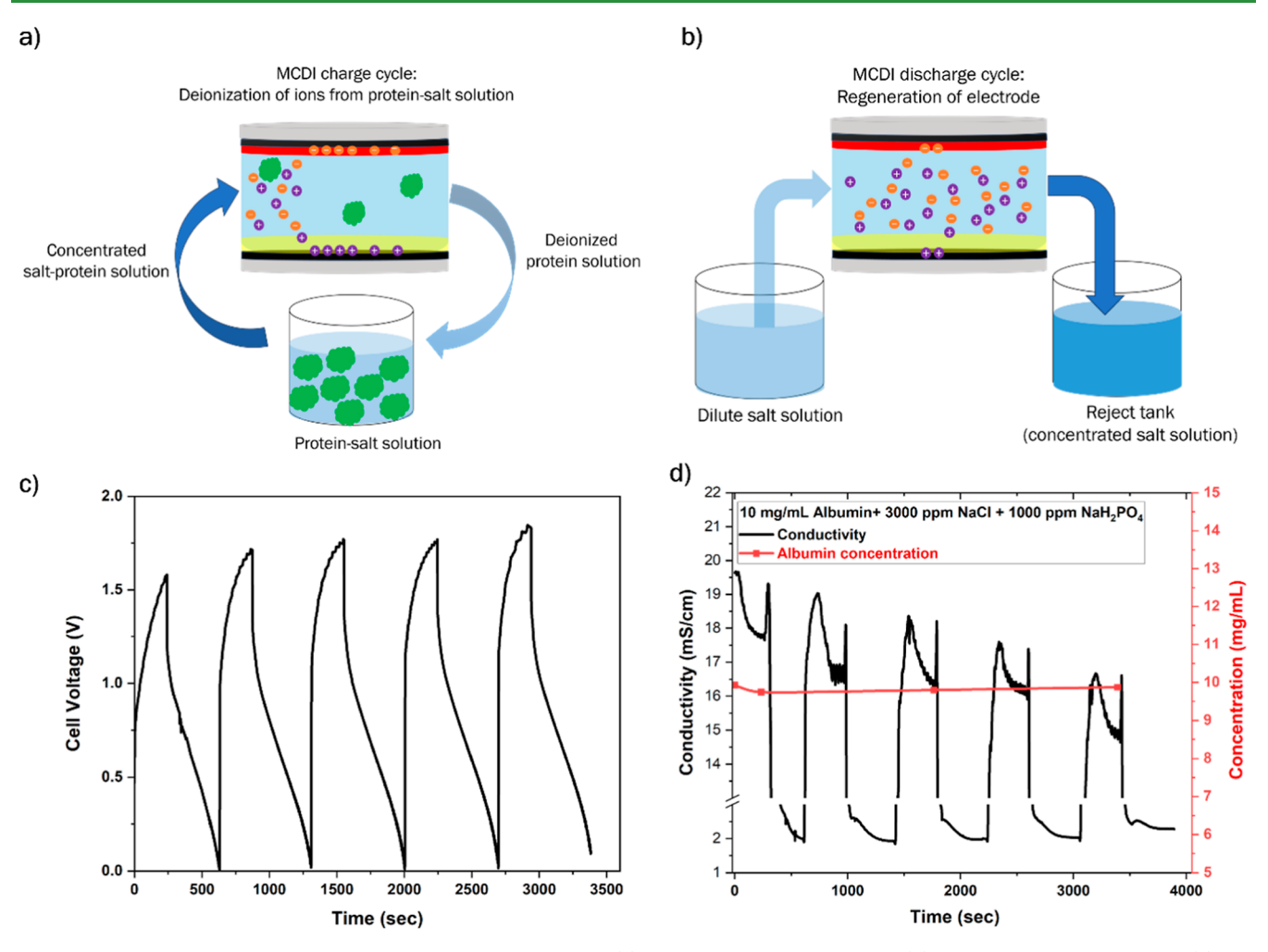


Figure 6. MCDI process flow schemes for the recirculation method for (a) charge cycle/deionization and (b) discharge/regeneration cycle. (c) Cell voltage vs time and (d) effluent conductivity vs time and HSA concentration versus time. Charge cycle conditions: feed: 10 mg/mL HSA +3000 ppm of NaCl +1000 ppm of NaH₂PO₄, current: 1.8 mA/cm^2 , time: 240 s. Discharge cycle conditions: feed: 250 ppm of NaCl, current: 0.6 mA/cm^2 , time: set to 0 V.

single-pass setup. Further deionization necessitates a large cell area, multiple cells, or recirculation of the process stream.

The last set of experiments recirculated the plasma protein stream, so a greater extent of deionization in the plasma protein solution can be achieved. Figure 6a conveys the recirculation strategy. For this experiment, the process stream consisted of 3000 ppm of NaCl mixed with 1000 ppm of NaH₂PO₄ and 10 mg mL⁻¹ of HSA feed. The process stream only passed through the MCDI unit during charge/deionization step. This stream was recirculated through the unit during the charge/deionization step. During discharge mode to regenerate the electrodes, the feed solution to the MCDI was changed to a low concentration of NaCl (250 ppm) feed (Figure 6b). Figure 6c,d presents the cell voltage versus time and the effluent conductivity versus time during charge-discharge cycling and the HSA concentration in the effluent. The conductivity of the plasma protein solution continued to decrease over multiple charge cycles (i.e., time). For instance, the initial conductivity of the first charge cycle was 19.5 mS/cm while the initial conductivity of fifth cycle was 16.3 mS/cm indicating ions are being removed from feed stream for every charge cycle. The ICP-OES data for chloride and phosphate concentrations with different charge cycles are provided in Table S8. Using the recirculation strategy, 28% of the salt in the plasma protein

solution was removed from the feed stream. During the recirculation, there was a negligible loss of protein (Figure 6d). As the salt is removed from the plasma protein solution, the cell voltage slightly climbs with each cycle as the concentration of ions in the solution is reduced. The incremental rise of the cell voltage can be attributed to the increase in the Ohmic resistance due to the reduction in the concentration of ionic charge carriers in the spacer channel. This problem can be partially mitigated by employing porous ionic conductors such as ionomer-coated nylon mesh as demonstrated in this article. Furthermore, another way of tackling this problem is by reducing the cell current density with each consecutive cycle so the cell voltage remains steady or to prevent it from getting too high where it spurs electrolysis or corrosion. Overall, the recirculation method for deionizing plasma protein solutions, as well as other ioncontaining solutions, has many advantages as it can lead to deeper deionization extents and it does not need multistage separation. Future work will look to optimize this process and compare against the advantages of a large cell and multiple MCDI units in series (or hybrid units in series electrodialysis followed by MCDI).

Assessment of Membrane Fouling. As indicated in Figure 5, there is a small amount (<3%) of loss of HSA during the MCDI operation. When juxtaposed against separation

platforms such as ion chromatography, which experiences significant fouling of the resin particles, it is paramount to assess whether the loss of HSA in MCDI leads to membrane fouling since the IEMs are the most expensive component in MCDI. We examined the surface of the IEMs before and after MCDI experiments with HSA solutions using SEM Figure S18a,b provides the SEM images of the AEM prior to and following deionization experiments (1000 magnifications). Likewise, Figure S18d,e depicts SEM images of CEM before and after deionization experiments with HSA solutions (at 1000 magnifications), respectively. Additionally, an in-depth SEM analysis at higher magnification was carried out for the AEM (Figure S18c) and CEM (Figure S18f) post-deionization experiments to evaluate protein fouling. We observed no aggregation or collection of the HSA on the IEM surface as shown in other reports.⁵¹ An additional investigation was conducted to assess the deionization of the HSA solution, both with and without the use of IEMs. Removing the IEMs from the deionization cell showed a lower drop in ionic conductivity when operating at constant current density indicating less deionization (Figure S12). Furthermore, there was about a 15 to 20% reduction in HSA in the effluent when there were no IEMs in the capacitive deionization unit (Figure S12). Figure S15 provides the UV-vis results of the effluent for the deionization experiments without IEMs. Overall, these results indicate that the IEMs shield the electrodes from fouling and ensure that the capacity of the electrodes is maintained after several cycles of deionization.

CONCLUSIONS

In this study, poly(phenylene alkylene) IEMs were tested in MCDI for the deionization of relatively high (up to 8000 ppm) sodium chloride and monosodium phosphate solutions in aqueous and protein solutions. Due to the high conductivity and low ASR values of poly(phenylene alkylene) IEMs when compared to commercial Fumasep IEMs, deionization performance metrics (such as ENAS and energy recovery) were improved. Additionally, Ohmic resistance in the spacer channel of the MCDI was ameliorated by incorporating poly(phenylene alkylene) ionomer-coated nylon meshes. The use of these porous ionic conductors also improved the ENAS and energy recovery. With respect to deionizing salty plasma protein solutions, an MCDI unit featuring highly conductive poly-(phenylene alkylene) IEMs and operating under recirculation removed 28% of the salt in the feed concentration while demonstrating 0-3% loss of HSA. SEM analysis indicated the absence of protein fouling on the membrane. Overall, MCDI is an effective electrochemical separation platform for deionizing plasma protein solutions.

ASSOCIATED CONTENT

Supporting Information

The Supporting Information is available free of charge at https://pubs.acs.org/doi/10.1021/acsami.3c16691.

Methods; synthesis of IEMs; membrane characterization; MCDI performance metric equations; NMR spectra of synthesized polymers used to make IEMs; MCDI process flow schemes; Nyquist plots for MCDI configurations with different IEMs and salt concentrations; cell voltage versus time and effluent conductivity versus time and albumin concentration vs time for MCDI vs CDI experiment; UV—visible calibration curve and deion-

ization experiment spectra; table for MCDI performance for different MCDI configuration. (1) poly(phenylene alkylene) vs Fumatech IEMs, (2) noncoated and ionomer coated MCDI configuration for different salt concentration, (3) HFR values from MCDI experiments, (4) concentration of HSA solution, ICP-OES data for MCDI experiments with (5) 5 mg/mL albumin, (6) 10 mg/mL albumin, (7) 20 mg/mL albumin and 10 mg/mL albumin (recirculation method) (PDF)

AUTHOR INFORMATION

Corresponding Author

Christopher G. Arges — Department of Chemical Engineering, Pennsylvania State University, University Park, Pennsylvania 16802, United States; Present Address: Transportation and Power Systems 556 Division, Argonne National Laboratory, Lemont, Illinois 557 60439, United States; orcid.org/0000-0003-1703-8323; Email: chris.arges@psu.edu, carges@anl.gov

Authors

Bharat Shrimant — Department of Chemical Engineering, Pennsylvania State University, University Park, Pennsylvania 16802, United States; orcid.org/0000-0002-1429-1182

Tanmay Kulkarni — Department of Chemical Engineering, Pennsylvania State University, University Park, Pennsylvania 16802, United States; oorcid.org/0000-0001-8911-1214

Mahmudul Hasan — Department of Chemical Engineering, Pennsylvania State University, University Park, Pennsylvania 16802, United States; oorcid.org/0000-0001-5462-3404

Charles Arnold – CSL Behring, Bradley, Illinois 60915, United

Nazimuddin Khan — CSL Behring, Bradley, Illinois 60915, United States

Abhishek N. Mondal – Donaldson Company Inc., Bloomington, Minnesota 55431, United States

Complete contact information is available at: https://pubs.acs.org/10.1021/acsami.3c16691

Notes

The authors declare no competing financial interest.

ACKNOWLEDGMENTS

This work was primarily supported through the Membrane Science, Engineering, and Technology (MAST) Center, which is funded by award # 1841474 from the NSF IUCRC program. This work was also partially supported by the Office of Naval Research (ONR), Award #N00014-22-1-2564. We thank Laura J. Liermann at the LIME Lab at Pennsylvania State University for performing ICP-OES analysis. We also thank Professor Christian Pester and Sarah Freeburne at Pennsylvania State University for the GPC analysis.

REFERENCES

ı

- (1) de la Rica, R.; Matsui, H. Applications of Peptide and Protein-based Materials in Bionanotechnology. *Chem. Soc. Rev.* **2010**, *39* (9), 3499–3509. 10
- (2) Xu, X.; Hu, J.; Xue, H.; Hu, Y.; Liu, Y.-n.; Lin, G.; Liu, L.; Xu, R.-a. Applications of Human and Bovine Serum Albumins in Biomedical Engineering: A Review. *Int. J. Biol. Macromol.* **2023**, 253, 126914.
- (3) Tao, H.-y.; Wang, R.-q.; Sheng, W.-j.; Zhen, Y.-s. The Development of Human Serum Albumin-based Drugs and Relevant

- Fusion Proteins for Cancer Therapy. *Int. J. Biol. Macromol.* **2021**, *187*, 24–34.
- (4) Liu, Z.; Chen, X. Simple Bioconjugate Chemistry Serves Great Clinical Advances: Albumin as a Versatile Platform for Diagnosis and Precision Therapy. *Chem. Soc. Rev.* **2016**, 45 (5), 1432–1456.
- (5) Knezevic-Maramica, I.; Kruskall, M. S. Intravenous Immune Globulins: An Update for Clinicians. *Transfusion* **2003**, 43 (10), 1460–1480. (accessed 2023/10/30)
- (6) Saab, W.; Seshadri, S.; Huang, C.; Alsubki, L.; Sung, N.; Kwak-Kim, J. A Systemic Review of Intravenous Immunoglobulin G Treatment in Women with Recurrent Implantation Failures and Recurrent Pregnancy Losses. *Am. J. Reprod. Immunol.* **2021**, 85 (4), No. e13395. (accessed 2023/10/30)
- (7) Farrugia, A.; Robert, P. Plasma Protein Therapies: Current and Future Perspectives. *Best Pract. Res. Clin. Haematol.* **2006**, 19 (1), 243–258
- (8) Adamski-Medda, D.; Nguyen, Q. T.; Dellacherie, E. Biospecific Ultrafiltration: A Promising Purification Technique for Proteins? *J. Membr. Sci.* 1981, 9 (3), 337–342.
- (9) Pires, I. S.; Palmer, A. F. Selective Protein Purification Via Tangential Flow Filtration Exploiting Protein-Protein Complexes to Enable Size-Based Separations. *J. Membr. Sci.* **2021**, *618*, 118712.
- (10) Andrew, S. M.; Titus, J. A.; Zumstein, L. Dialysis and Concentration of Protein Solutions. *Curr. Protoc. Toxicol.* **2001**, *10* (1), A.3H.1–A.3H.5. (accessed 2023/10/30)
- (11) Knudsen, H. L.; Fahrner, R. L.; Xu, Y.; Norling, L. A.; Blank, G. S. Membrane Ion-exchange Chromatography for Process-scale Antibody Purification. *J. Chromatogr.*, A **2001**, 907 (1–2), 145–154.
- (12) Duong-Ly, K. C.; Gabelli, S. B. Using Ion Exchange Chromatography to Purify a Recombinantly Expressed Protein. In *Methods in Enzymology*, Lorsch, J., Ed.; Academic Press, 2014; Vol. 541, Chapter 8; pp 95–103.
- (13) Emin, C.; Kurnia, E.; Katalia, I.; Ulbricht, M. Polyarylsulfone-based Blend Ultrafiltration Membranes with Combined Size and Charge Selectivity for Protein Separation. Sep. Purif. Technol. 2018, 193, 127–138
- (14) Saxena, A.; Tripathi, B. P.; Kumar, M.; Shahi, V. K. Membrane-based Techniques for the Separation and Purification of Proteins: An Overview. *Adv. Colloid Interface Sci.* **2009**, *145* (1–2), 1–22.
- (15) Ghosh, R. Separation of Human Albumin and IgG by a Membrane-based Integrated Bioseparation Technique Involving Simultaneous Precipitation, Microfiltration and Membrane Adsorption. J. Membr. Sci. 2004, 237 (1–2), 109–117.
- (16) Ghosh, R. Protein Separation Using Membrane Chromatography: Opportunities and Challenges. *J. Chromatogr., A* **2002**, 952 (1–2), 13–27.
- (17) Kreusser, J.; Hasse, H.; Jirasek, F. Adsorption of Bovine Serum Albumin on a Mixed-mode Resin Influence of Salts and The pH Value. *Adsorption* **2023**, 29 (3–4), 163–176.
- (18) Niu, C.; Li, X.; Dai, R.; Wang, Z. Artificial Intelligence-incorporated Membrane Fouling Prediction for Membrane-based Processes in the Past 20 Years: A Critical Review. *Water Res.* **2022**, *216*, 118299.
- (19) Alkhadra, M. A.; Su, X.; Suss, M. E.; Tian, H.; Guyes, E. N.; Shocron, A. N.; Conforti, K. M.; de Souza, J. P.; Kim, N.; Tedesco, M.; et al. Electrochemical Methods for Water Purification, Ion Separations, and Energy Conversion. *Chem. Rev.* **2022**, *122* (16), 13547–13635.
- (20) Gao, F.; Wang, L.; Wang, J.; Zhang, H.; Lin, S. Nutrient Recovery from Treated Wastewater by a Hybrid Electrochemical Sequence Integrating Bipolar Membrane Electrodialysis and Membrane Capacitive Deionization. *Environ. Sci.: Water Res. Technol.* **2020**, 6 (2), 383–391.
- (21) Kim, N.; Jeon, J.; Chen, R.; Su, X. Electrochemical Separation of Organic Acids and Proteins for Food and Biomanufacturing. *Chem. Eng. Res. Des.* **2022**, *178*, 267–288.
- (22) Arana Juve, J.-M.; Christensen, F. M. S.; Wang, Y.; Wei, Z. Electrodialysis for Metal Removal and Recovery: A Review. *Chem. Eng. J.* 2022, 435, 134857.

- (23) Kim, Y.-J.; Choi, J.-H. Enhanced Desalination Efficiency in Capacitive Deionization with an Ion-selective Membrane. *Sep. Purif. Technol.* **2010**, *71* (1), 70–75.
- (24) Kulkarni, T.; Al Dhamen, A. M. I.; Bhattacharya, D.; Arges, C. G. Bipolar Membrane Capacitive Deionization for pH-Assisted Ionic Separations. *ACS ES&T Eng.* **2023**, *3*, 2171–2182.
- (25) Kim, N.; Jeon, J.; Elbert, J.; Kim, C.; Su, X. Redox-mediated Electrochemical Desalination for Waste Valorization in Dairy Production. *Chem. Eng. J.* **2022**, 428, 131082.
- (26) Jordan, M. L.; Kokoszka, G.; Gallage Dona, H. K.; Senadheera, D. I.; Kumar, R.; Lin, Y. J.; Arges, C. G. Integrated Ion-Exchange Membrane Resin Wafer Assemblies for Aromatic Organic Acid Separations Using Electrodeionization. ACS Sustainable Chem. Eng. 2023, 11 (3), 945–956.
- (27) Hülber-Beyer, É.; Bélafi-Bakó, K.; Nemestóthy, N. Low-waste Fermentation-derived Organic Acid Production by Bipolar Membrane Electrodialysis—An Overview. *Chem. Pap.* **2021**, *75* (10), 5223—5234.
- (28) Gausmann, M.; Kocks, C.; Pastoors, J.; Büchs, J.; Wierckx, N.; Jupke, A. Electrochemical pH-T-Swing Separation of Itaconic Acid for Zero Salt Waste Downstream Processing. *ACS Sustainable Chem. Eng.* **2021**, *9* (28), 9336–9347.
- (29) Fritz, P. A.; Boom, R. M.; Schroën, C. Electrochemically Driven Adsorptive Separation Techniques: From Ions to Proteins and Cells in Liquid Streams. *Sep. Purif. Technol.* **2021**, *274*, 118754.
- (30) Rottiers, T.; Ghyselbrecht, K.; Meesschaert, B.; Van der Bruggen, B.; Pinoy, L. Influence of the Type of Anion Membrane on Solvent Flux and Back Diffusion in Electrodialysis of Concentrated NaCl Solutions. *Chem. Eng. Sci.* **2014**, *113*, 95–100.
- (31) Liu, H.; She, Q. Influence of Membrane Structure-dependent Water Transport on Conductivity-permselectivity Trade-off and Salt/Water Selectivity in Electrodialysis: Implications for Osmotic Electrodialysis using Porous Ion Exchange Membranes. *J. Membr. Sci.* **2022**, 650, 120398.
- (32) Rommerskirchen, A.; Roth, H.; Linnartz, C. J.; Egidi, F.; Kneppeck, C.; Roghmans, F.; Wessling, M. Mitigating Water Crossover by Crosslinked Coating of Cation-Exchange Membranes for Brine Concentration. *Adv. Mater. Technol.* **2021**, *6* (10), 2100202. (accessed 2024/01/31)
- (33) Zhao, Y.; Wang, Y.; Wang, R.; Wu, Y.; Xu, S.; Wang, J. Performance Comparison and Energy Consumption Analysis of Capacitive Deionization and Membrane Capacitive Deionization Processes. *Desalination* **2013**, 324, 127–133.
- (34) Biesheuvel, P. M.; van der Wal, A. Membrane Capacitive Deionization. *J. Membr. Sci.* **2010**, 346 (2), 256–262.
- (35) Sun, K.; Tebyetekerwa, M.; Wang, C.; Wang, X.; Zhang, X.; Zhao, X. S. Electrocapacitive Deionization: Mechanisms, Electrodes, and Cell Designs. *Adv. Funct. Mater.* **2023**, 33 (18), 2213578. (accessed 2023/08/24)
- (36) Porada, S.; Zhao, R.; van der Wal, A.; Presser, V.; Biesheuvel, P. M. Review on the Science and Technology of Water Desalination by Capacitive Deionization. *Prog. Mater. Sci.* **2013**, *58* (8), 1388–1442.
- (37) Noh, S.; Jeon, J. Y.; Adhikari, S.; Kim, Y. S.; Bae, C. Molecular Engineering of Hydroxide Conducting Polymers for Anion Exchange Membranes in Electrochemical Energy Conversion Technology. *Acc. Chem. Res.* **2019**, 52 (9), 2745–2755.
- (38) Palakkal, V. M.; Rubio, J. E.; Lin, Y. J.; Arges, C. G. Low-Resistant Ion-Exchange Membranes for Energy Efficient Membrane Capacitive Deionization. *ACS Sustainable Chem. Eng.* **2018**, *6* (11), 13778–13786.
- (39) Palakkal, V. M.; Jordan, M. L.; Bhattacharya, D.; Lin, Y. J.; Arges, C. G. Addressing Spacer Channel Resistances in MCDI Using Porous and Pliable Ionic Conductors. *J. Electrochem. Soc.* **2021**, *168* (3), 033503. (accessed 2023/08/24)
- (40) Lee, W.-H.; Park, E. J.; Han, J.; Shin, D. W.; Kim, Y. S.; Bae, C. Poly(terphenylene) Anion Exchange Membranes: The Effect of Backbone Structure on Morphology and Membrane Property. *ACS Macro Lett.* **2017**, *6* (5), 566–570.
- (41) Pagels, M. K.; Adhikari, S.; Walgama, R. C.; Singh, A.; Han, J.; Shin, D.; Bae, C. One-Pot Synthesis of Proton Exchange Membranes

- from Anion Exchange Membrane Precursors. ACS Macro Lett. 2020, 9 (10), 1489–1493.
- (42) Galvan, V.; Shrimant, B.; Bae, C.; Prakash, G. K. S. Ionomer Significance in Alkaline Direct Methanol Fuel Cell to Achieve High Power with a Quarternized Poly(terphenylene) Membrane. *ACS Appl. Energy Mater.* **2021**, *4* (6), 5858–5867.
- (43) Kitto, D.; Kamcev, J. The Need for Ion-exchange Membranes with High Charge Densities. *J. Membr. Sci.* **2023**, *677*, 121608.
- (44) Lee, W.-H.; Kim, Y. S.; Bae, C. Robust Hydroxide Ion Conducting Poly(biphenyl alkylene)s for Alkaline Fuel Cell Membranes. ACS Macro Lett. 2015, 4 (8), 814–818.
- (45) Xu, Y.; Jiang, T.; Zhang, X.; Cao, G.; Yang, L.; Wei, H.; Zhou, H. Poly(arylene alkylene)-Based Ion-Exchange Polymers for Enhancing Capacitive Desalination Capacity and Electrode Stability. *Ind. Eng. Chem. Res.* **2023**, *62* (36), 14601–14610.
- (46) Gamaethiralalage, J. G.; Singh, K.; Sahin, S.; Yoon, J.; Elimelech, M.; Suss, M. E.; Liang, P.; Biesheuvel, P. M.; Zornitta, R. L.; de Smet, L. C. P. M. Recent Advances in Ion Selectivity with Capacitive Deionization. *Energy Environ. Sci.* **2021**, *14* (3), 1095–1120.
- (47) Zhang, J.; Tang, L.; Tang, W.; Zhong, Y.; Luo, K.; Duan, M.; Xing, W.; Liang, J. Removal and Recovery of Phosphorus from Lowstrength Wastewaters by Flow-electrode Capacitive Deionization. *Sep. Purif. Technol.* **2020**, 237, 116322.
- (48) Chrispim, M. C.; Scholz, M.; Nolasco, M. A. Phosphorus Recovery from Municipal Wastewater Treatment: Critical Review of Challenges and Opportunities for Developing Countries. *J. Environ. Manage.* **2019**, 248, 109268.
- (49) Ge, Z.; Chen, X.; Huang, X.; Ren, Z. J. Capacitive Deionization for Nutrient Recovery from Wastewater with Disinfection Capability. *Environ. Sci.: Water Res. Technol.* **2018**, *4* (1), 33–39.
- (50) Kumar, M.; Jaiswal, V. D.; Pangam, D. S.; Bhatia, P.; Kulkarni, A.; Dongre, P. M. Biophysical Study of DC Electric Field Induced Stable Formation of Albumin-gold Nanoparticles Corona and Curcumin Binding. *Spectrochim. Acta, Part A* **2024**, *305*, 123469.
- (51) Wang, Y.; Zheng, X.; Li, D.; Tian, J.; Wu, H.; Zhang, Y. Comparison of Membrane Fouling Induced by Protein, Polysaccharide and Humic Acid under Sodium and Calcium Ionic Conditions. *Desalination* **2023**, *548*, 116236.